

## Live attenuated coronavirus vaccines deficient in N7-Methyltransferase activity induce both humoral and cellular immune responses in mice

Zhen Zhang <sup>a,\*</sup>, Qianyun Liu <sup>a,\*</sup>, Ying Sun<sup>b</sup>, Jiali Li<sup>a</sup>, Jiejie Liu<sup>a</sup>, Ruangang Pan<sup>a</sup>, Liu Cao<sup>c</sup>, Xianying Chen<sup>a</sup>, Yingjian Li<sup>a</sup>, Yuzhen Zhang<sup>d</sup>, Ke Xu<sup>a</sup>, Deyin Guo<sup>c</sup>, Li Zhou <sup>a,d</sup>, Ke Lan <sup>a</sup> and Yu Chen <sup>a</sup>

<sup>a</sup>State Key Laboratory of Virology, Modern Virology Research Center, Institute for Vaccine Research, RNA Institute, College of Life Sciences, Wuhan University, Wuhan, People's Republic of China; <sup>b</sup>School of Chinese Medicine (Zhongjing School), Henan University of Chinese Medicine, Zhengzhou, People's Republic of China; <sup>c</sup>Center for Infection & Immunity Study, School of Medicine, Sun Yat-sen University, Guangzhou, People's Republic of China; <sup>d</sup>Animal Bio-Safety Level III Laboratory at Center for Animal Experiments, Wuhan University School of Medicine, Wuhan, People's Republic of China

### ABSTRACT

Coronaviruses (CoVs) can infect a variety of hosts, including humans, livestock and companion animals, and pose a serious threat to human health and the economy. The current COVID-19 pandemic, which is caused by severe acute respiratory syndrome coronavirus 2 (SARS-CoV-2), has killed millions of people. Unfortunately, effective treatments for CoVs infection are still lacking, suggesting the importance of coronavirus vaccines. Our previous work showed that CoV nonstructural protein 14 (nsp14) functions as (guanine-N7)-methyltransferase (N7-MTase), which is involved in RNA cap formation. Moreover, we found that N7-MTase is well conserved among different CoVs and is a universal target for developing antivirals against CoVs. Here, we show that N7-MTase of CoVs can be an ideal target for designing live attenuated vaccines. Using murine hepatitis virus strain A59 (MHV-A59), a representative and well-studied model of coronaviruses, we constructed N7-MTase-deficient recombinant MHV D330A and Y414A. These two mutants are highly attenuated in mice and exhibit similar replication efficiency to the wild-type (WT) virus in the cell culture. Furthermore, a single dose immunization of D330A or Y414A can induce long-term humoral immune responses and robust CD4<sup>+</sup> and CD8<sup>+</sup> T cell responses, which can provide full protection against the challenge of a lethal-dose of MHV-A59. Collectively, this study provides an ideal strategy to design live attenuated vaccines for coronavirus by abolishing viral RNA N7-MTase activity. This approach may apply to other RNA viruses that encode their own conservative viral N7-methyltransferase.

**ARTICLE HISTORY** Received 24 June 2021; Revised 30 July 2021; Accepted 1 August 2021

**KEYWORDS** Coronavirus; vaccine; N7-Methyltransferase; nsp14; cap structure

### Introduction

Coronaviruses are enveloped positive-sense single-stranded RNA viruses. They can infect different hosts, including humans, livestock, mice, bats and other wild animals, and pose a serious threat to human health, public safety and the economy [1]. According to the International Committee on Taxonomy of Viruses (ICTV) classification, CoVs belong to subfamily Coronavirinae in the family Coronaviridae of the order Nidovirales [2]. Coronavirinae is further subdivided into four genera: *Alphacoronavirus*, *Beta*-*coronavirus*, *Gammacoronavirus* and *Deltacoronavirus*. The former two infect only mammals, while the latter two primarily infect birds [3]. Since the early 1930s, a variety of domestic diseases have been found related to CoV infections. For instance, infectious bronchitis virus (IBV) usually causes avian

infectious bronchitis accompanied by upper respiratory symptoms and urinary and reproductive system failures, resulting in low production rates, egg drop, and death in chickens [4]. Several porcine CoVs, such as transmissible gastroenteritis virus (TGEV), porcine respiratory coronavirus (PRCV), porcine epidemic diarrhoea virus (PEDV), porcine deltacoronavirus (PDCoV), and emerging swine acute diarrhoea syndrome-coronavirus (SADS-CoV), have widely circulated in pigs worldwide and caused severe gastrointestinal diseases in suckling piglets with high mortality, culminating in major losses to the pork industry [5,6]. Simultaneously, MHV, a betacoronavirus that infects mice and induces disease in several organ systems, was widely studied to understand the pathogenic biology of coronavirus [7]. In humans, some low pathogenic CoVs, such as HCoV-229E and

**CONTACT** Yu Chen  [chenyu@whu.edu.cn](mailto:chenyu@whu.edu.cn)  State Key Laboratory of Virology, Modern Virology Research Center, Institute for Vaccine Research, RNA Institute, College of Life Sciences, Wuhan University, Wuhan 430072, People's Republic of China

\*These authors contributed equally.

 Supplemental data for this article can be accessed at <https://doi.org/10.1080/22221751.2021.1964385>.

© 2021 The Author(s). Published by Informa UK Limited, trading as Taylor & Francis Group, on behalf of Shanghai Shangyixun Cultural Communication Co., Ltd  
This is an Open Access article distributed under the terms of the Creative Commons Attribution License (<http://creativecommons.org/licenses/by/4.0/>), which permits unrestricted use, distribution, and reproduction in any medium, provided the original work is properly cited.

HCoV-OC43, are widely spread among people but primarily cause self-limiting disease with mild symptoms [8]. Remarkably, three highly transmissible and pathogenic zoonotic betacoronaviruses, namely, severe acute respiratory syndrome coronavirus (SARS-CoV), Middle East respiratory syndrome coronavirus (MERS-CoV), and SARS-CoV-2 have emerged in humans over the last two decades [9–13]. Infection with these viruses can cause fatal respiratory illness, making emerging coronaviruses a new public health concern [14]. SARS-CoV and MERS-CoV caused local outbreaks with high morbidity and mortality in 2003 and 2012, respectively, whereas SARS-CoV-2 has resulted in the COVID-19 pandemic [14,15]. As of June 2021, there have been 170 million confirmed cases of COVID-19, including at least 3.69 million deaths according to the latest report from the WHO (<https://covid19.who.int/>).

Since the outbreak of the emerging coronavirus, much progress has been made on coronavirus biology. The coronavirus virion consists of four structural proteins – spike (S), envelope (E), membrane (M), nucleocapsid (N) – and a positive-sense single-stranded RNA (+ssRNA) ( $\approx 30$  kb) genome with a 5'-cap structure and 3'-poly-A tail encapsulated in the virus particle. Two-thirds of the 5'-genome contains open reading frame 1a (ORF1a) and ORF1b, and can be directly translated into two large polyproteins, 1a/1ab (pp1a/pp1ab), which are cleaved into 15 or 16 non-structural proteins (nsp) to form the replication-transcription complex (RTC) in double-membrane vesicles (DMVs) [1,16–18]. The remaining third of the 3'-genome encodes structural and virus-specific accessory proteins, which are expressed from subgenomic RNAs (sgRNAs) synthesized through the discontinuous viral transcription process [3,19,20]. During the viral life cycle, CoVs primarily enter cells through the interaction between S protein and specific receptors. They subsequently utilize cellular machinery to translate their nsps, which conduct replication of genomic RNA and transcription of sgRNAs to produce full-length copies and viral proteins [3]. It is noteworthy that the mature 5'-cap structure, which harbours methylation at the N7 position of the capping guanylate and 2'-O position of the first and second nucleotides, is important for RNA stability and efficient translation during the replication of CoVs [21]. Besides, coronavirus ribose 2'-O-methylation allows the viral RNA to evade the recognition of host RNA sensors, such as Mda5, thus perturbing the host's innate immune responses [22]. For CoVs, cap formation requires the following enzymes: RNA triphosphatase (TPase), RNA guanylyltransferase (GTase), N7-MTase, and 2'-O-MTase. We previously showed that CoV nsp14 functions as N7-MTase to produce a cap-0 structure, which is the basis of the cap-1 structure that mediates immune escape [22,23].

Moreover, we showed that the N7-MTase is well conserved among different CoVs, and is a universal target for developing antivirals against CoVs [24,25]. Meanwhile, the critical amino acid residues essential for N7-MTase activity were also identified. However, the details of different residues on viral replication and pathogenicity are still not well understood.

Here, we introduced single amino acid substitution at conserved position D330 or Y414 of MHV nsp14 and generated two MHV N7-MTase mutant virus D330A and Y414A by a reverse genetic system. We found that the two mutants were genetically stable and slightly attenuated in the cell culture, but were extremely attenuated in virulence and pathogenicity in mice. Furthermore, we showed that a single dose of D330A or Y414A immunization could elicit long-term humoral immune responses that last for at least 48 weeks. More importantly, the immunization could also induce robust CD4<sup>+</sup> and CD8<sup>+</sup> T cell responses and provide full protection against lethal challenge with WT MHV-A59 strains in mice. This study demonstrates the feasibility of using N7-MTase as a target to design live attenuated vaccines. Considering the conservation of N7-MTase in different CoVs, this strategy is promising for applications to develop live attenuated vaccines against new emerging CoVs, especially CoVs circulating in livestock.

## Materials and methods

### Cells and animals

CV-1, BHK-21-MHV-N, HeLa-D980R, 17CL-1, L2 and Neuro 2a cells were cultured at 37°C with 5% CO<sub>2</sub> in Dulbecco modified Eagle's medium (DMEM, Gibco) supplemented with 10% foetal bovine serum (FBS, Gibco) and 1% penicillin/streptomycin (Gibco). Four-week-old SPF C57BL/6 mice were purchased from Beijing Vital River Laboratory Animal Technology Co. Ltd. (Beijing, China). All mice were maintained in individually ventilated cages (IVC) in an animal biosafety level 2 (ABSL-2) facility and received care in compliance with international legal requirements throughout the experiments.

### Protein expression and purification

The recombinant plasmids encoding MHV nsp14, MHV nsp14 mutants or SARS-CoV-2 nsp14 were constructed as previously described [24]. They were then transformed into *Escherichia coli* BL21. Cells were cultivated at 37°C in a shaker incubator and induced with 0.4 mM isopropyl  $\beta$ -D-thiogalactoside (IPTG) when OD<sub>600</sub> nm reached 0.8. Cells were harvested after induction at 16°C for 16 h, and lysed by enzymolysis in 50 mM NaH<sub>2</sub>PO<sub>4</sub> (pH 8.0), 300 mM NaCl, 10 mM imidazole, 5% (vol/vol) glycerol, 0.4

mg/mL lysosome, 1 mM PMSF, and 0.02% (v/v) NP40, and DNAs and RNAs in the lysate were digested by 10 mM MgCl<sub>2</sub>, 5 µg/mL DNase I and 10 µg/mL RNase A. After centrifugation, recombinant protein was purified using Ni-affinity resin (Novagen) with different concentrations of imidazole for washing and elution, which was followed by chromatography using a Superdex 200 column of AKTA pure GE. All nsp14 mutants were expressed and purified as described above.

### **N7-MTase activity assay**

RNA (5'-GATTTAAGTGAATAGCTTGG-3') was synthesized in vitro (RiboMAX™ Large Scale RNA Production System-T7, Promega) and then capped by vaccine capping system (NEB). Purified proteins and 1 µM 5' capping RNA substrate were added to a reaction system which contained 1 mM <sup>3</sup>H-SAM, 40 mM Tris (pH 8.0), 5 mM DTT, and 1U RNase inhibitor. After being incubated at 37°C for 1 h, the RNA was purified by DEAE Sephadex A-25 (GE) and added to a liquid scintillation cocktail to test its radioactivity by Liquid Scintillation Analyzer (PerkinElmer).

### **Construction of MHV-A59 N7-MTase mutants**

Recombinant vaccinia virus inf-1 (vMHV-inf-1) containing a cloned, full-length MHV-A59 cDNA and recombinant vaccinia virus vMHV-nsp14-gpt-in, in which the MHV-A59 nsp14 gene was replaced by the *E. coli* guanine-phosphoribosyl-transferase (GPT) gene were kindly provided by Prof. Chang Guohui. The MHV-A59 nsp14 gene (nucleotides 17,634–17,660) was cloned from vMHV-inf-1 DNA by standard PCR, and nsp14 mutant genes containing mutations for D330A or Y414A were generated and inserted into pMD18-T to produce recombinant plasmids. Next, we used a reverse genetic system to generate MHV-A59 N7-MTase mutant viruses as described previously [26]. Briefly, monolayer CV-1 cells were infected with vMHV-nsp14-gtp-in, followed by transfection of the recombinant plasmids using Lipofectamine 2000 transfection reagent (Invitrogen). Two or three days later, the cells were harvested and recombinant vaccinia viruses were isolated by three rounds of plaque purification with GPT-positive or GPT-negative selection as described previously [27]. GPT-positive clones were selected by three rounds of plaque purification on CV-1 cells in the presence of xanthine, hypoxanthine and mycophenolic acid, while GPT-negative clones, in which the GPT gene was replaced by the nsp14 mutant gene, were selected by three rounds of plaque purification on D980R cells in the presence of 6-thioguanine. Recombinant MHV-A59 nsp14 mutants were rescued on a modified BHK-21 cell line expressing the MHV-A59 N protein. The cDNA of recombinant vaccinia

viruses vMHV-inf-1 or vMHV-nsp14-mutant were extracted, purified and cleaved, and the resulting DNA products were used as templates for the transcription of MHV-A59 RNA, which was transfected into BHK-21-MHV-N cells. Following transfection, the transfected BHK-MHV-N cells were mixed with 17Cl-1 cells at a ratio of 1/4. At one to two days post transfection, cell culture supernatants were harvested, and recombinant MHV-A59 N7-MTase mutants D330A and Y414A, as well as recombinant MHV-A59 wild type (WT), were plaque purified three times, and a single plaque was used to produce a virus stock. Viruses were aliquoted and stored at –80°C.

### **Viral plaque assay**

MHV viruses were amplified on Neuro 2a cells and titrated on L2 cells by plaque assay. Briefly, serial 10-fold dilutions of viruses were added into monolayer L2 cells. After 1 h of adsorption at 37°C, the inoculum was removed and cells were supplemented with DMEM containing 1.0% methylcellulose and 5% FBS. Plates were incubated for 2 days until obvious plaques can be observed. Cells were stained with 1% crystal violet for 12 h. Plaques were counted and viral titres were expressed as PFU/mL.

### **Genetic stability of mutants**

To examine the genetic stability of mutants, viruses were separately passaged on Neuro 2a cells for 10 rounds. Six-well plates were seeded with Neuro 2a cells and viruses P0 were added to infect Neuro 2a cells. At 16 h post infection (hpi), culture fluids were harvested and transferred to a new well containing fresh Neuro 2a cells. After 10 rounds of such passing, cell total RNA was extracted and cDNA was obtained using reverse transcription. The DNA segment encoding nsp14 was amplified and the products were subjected to DNA sequencing.

### **Virulence of mutants in vivo**

For the virulence and pathogenesis study, 4-week-old male SPF C57BL/6 mice were anaesthetized and followed by intrahepatic (i.h.) inoculation with 100 µL of DMEM containing 2×10<sup>6</sup> PFU MHV-A59 WT virus or N7-MTase mutants, while 100 µL of DMEM was i.h. inoculated as a mock control. Infected mice were monitored for body weight loss, clinical signs of disease and mortality daily. At 1, 2, 5 days post infection (dpi), mice were sacrificed and sera were collected for detection of alanine aminotransferase (ALT) levels according to the manufacturer's recommendations. Liver was also collected for viral load determination and histological analysis.

### Vaccination and challenge of mice

For immunization, 4-week-old female C57BL/6 mice were subcutaneously vaccinated with a 100  $\mu$ L volume containing either  $5 \times 10^5$  PFU MHV-A59 WT, D330A, Y414A or DMEM mock. At 2 weeks post immunization (wpi) and 4 wpi, sera of infected animals were collected for IgG and neutralization antibody measurement. At 4 wpi, mice were sacrificed and spleens were removed to prepare single-cell suspensions for cytokine assay. To test the duration that neutralizing antibodies persist for, mice were kept for 48 weeks and sera were collected every 4 weeks. Mice were challenged with  $2 \times 10^7$  PFU MHV-A59 by i.h. at 30 days post infection (dpi), then body weight and survival were monitored. The liver was then removed for viral titre determination and histological analysis.

### IgG titre measurement

An enzyme-linked immunosorbent assay (ELISA) was conducted to measure the IgG antibody titre against MHV in the sera. Briefly, twofold serially diluted sera were added to 96-well microtiter plates precoated with heat-inactivated MHV-A59. The plates were incubated at 37°C for 2 h, followed by five washes with PBST. After that, AP-conjugated goat anti-mouse IgG antibodies (Southern Biotech) were added and incubated at 37°C for 1 h. Finally, the substrate 4-Nitrophenyl phosphate disodium salt hexahydrate (Sigma) was added to the plates, and 45 min later the absorbance at 405 nm was measured by an ELISA plate reader (Tecan, San Jose, CA). Endpoint titres were defined as the lowest dilution of serum in which binding was twofold greater than the mean binding observed in the negative controls.

### Plaque reduction neutralization test

MHV-specific neutralizing antibody titres in immunized mouse sera were measured by a standard 50% plaque reduction neutralization test (PRNT<sub>50</sub>). Briefly, twofold serial dilutions of heat-inactivated sera were mixed with equal volumes of approximately 100 infectious MHV-A59 and incubated at 37°C for 1 h. The resulting virus-serum mixtures were then transferred to confluent L2 cells, followed by 1 h of incubation. L2 cells were grown in 1.0% methylcellulose medium and stained as described above. Plaques were counted and PRNT<sub>50</sub> values were calculated by the Reed-Muech method.

### Splenocyte stimulation and cytokine assay

Splenocytes of vaccinated mice were prepared and stimulated with WT MHV virus *in vitro* and the production of cytokines was analysed by FACS and

ELISA. Briefly, approximately  $5 \times 10^6$  splenocytes were stimulated with  $5 \times 10^6$  live WT MHV-A59. For ELISA, cell supernatants were directly collected at 48 hpi to detect the secretion of interferon- $\gamma$  (IFN- $\gamma$ ), interleukin-2 (IL-2), IL-10, and IL-4. For intracellular cytokine staining, brefeldin A (Sigma) at a final concentration of 5 ng/mL was added into wells to block protein transport during the final 5 h of stimulation. After that, cells were stained with anti-mouse mAbs CD3-PERCP (Biolegend), CD4-FITC (Biolegend), or CD8-APC (4A Biotech) for 30 min at 4°C, which was followed by treatment with fixation buffer and permeabilization buffer in accordance with the manufacturer's protocol (Biolegend). Then, either PE-conjugated anti-IFN- $\gamma$  antibody or an isotype control of rat IgG1 (Biolegend) was added to cells. The stained samples were analysed with flow cytometer FACSCalibur (BD Biosciences) and the data were analysed by FlowJo software.

### Statistical analysis

All experiments were performed at least three times and the results were measured as a mean  $\pm$  SD or mean  $\pm$  SEM. Student's *t*-tests were used to measure statistical differences between samples using GraphPad Prism 7 (GraphPad Software Inc, USA), in which  $P < 0.05$  was considered a statistically significant difference.

## Results

### Construction and characterization of MHV N7-MTase mutants

In previous studies, we showed that CoV nsp14 possesses guanine N7-MTase activity coupled with known ExoN activity, and the N7-MTase is highly conserved among different CoVs [23,25,28]. Further structure-function analysis suggested that the single amino acid substitution D331A, which is in the DxG S-adenosyl-L-methionine (SAM)-binding motif, and Y420A, which is in the supporting structure of the SAM-binding pocket, can affect the SAM-binding affinity of SARS-CoV N7-MTase and abolish its N7-methylation activity *in vitro* [24]. Alignment of nsp14 amino acid sequences showed that the two residues are also highly conserved among different CoVs (supplementary Figure S1). To verify the effects of these conserved key residues on MHV N7-MTase enzymatic activity, we introduced the two mutations into MHV-A59 nsp14 and expressed MHV nsp14 mutant protein D330A as well as Y414A in *E. coli* cells (Figure 1(A)), followed by an N7-MTase activity test in biochemical MTase assays as described previously [24]. In this test, <sup>3</sup>H-labeled methyl donor [<sup>3</sup>H]-SAM was used and the radiolabeled methyl

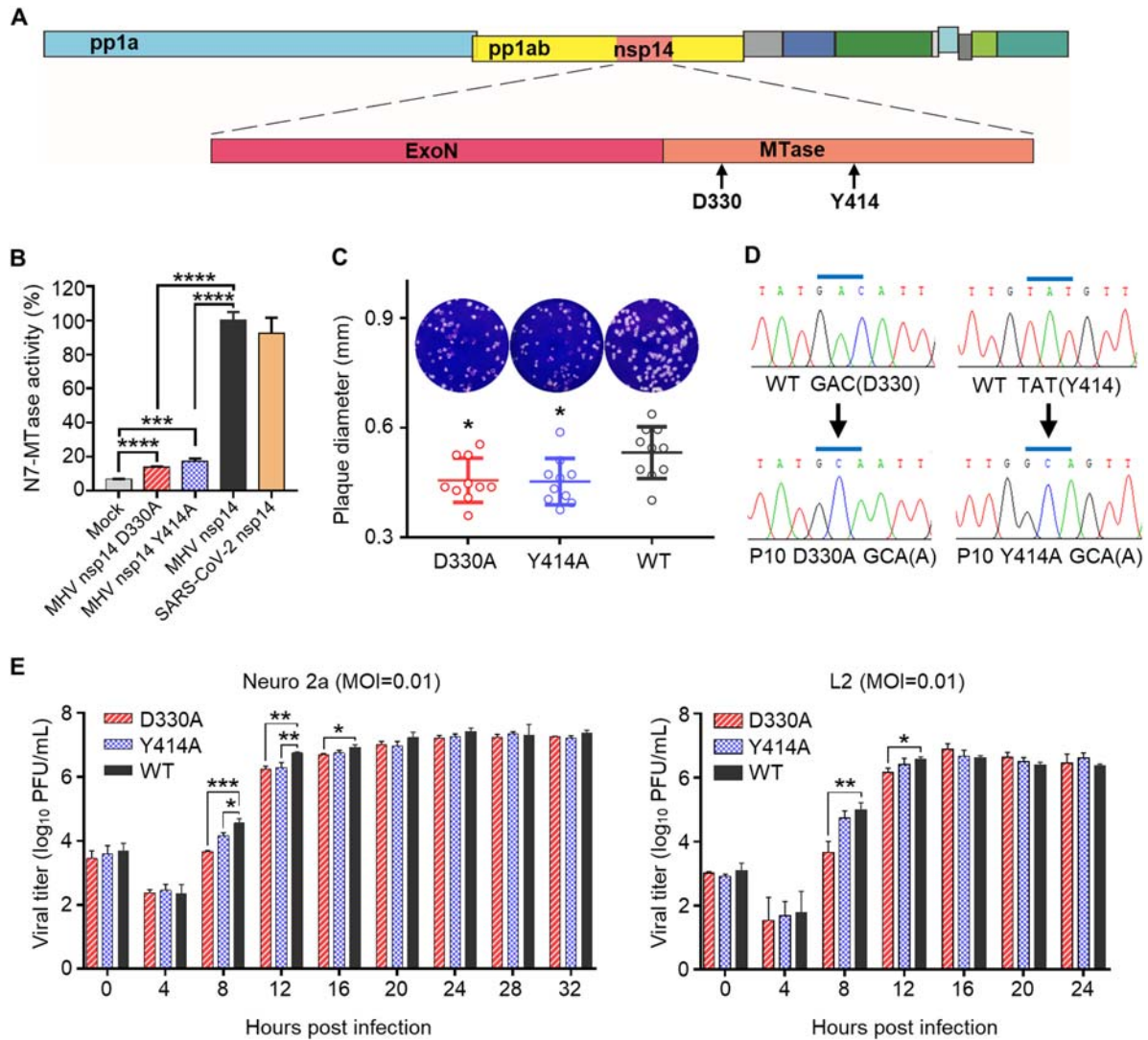


**Figure 1.** Construction and characterization of MHV nsp14 N7-MTase mutants. (A) Structure of MHV-A59 genome. The mutation sites in nsp14 N7-MTase domain are shown. (B) N7-MTase activity assay for nsp14 and its mutants in vitro. The N7-MTase activity of WT MHV nsp14 was set as 100%. Means with SD are shown ( $n = 3$ ). (C) Plaque morphology of mutant D330A, Y414A and WT virus at passage 10 (P10). Viruses were passaged on Neuro 2a cells for 10 rounds, and the resulting P10 viruses were examined by plaque assay. The diameters of representative plaques were measured and are shown as means with SD ( $n = 10$ ). (D) The D330A and Y414A mutants were maintained after 10 rounds of passage. The cDNA fragments encoding nsp14 of P10 viruses were amplified by RCR and the products were sequenced. (E) One-step replication curves of D330A, Y414A, and WT virus were measured on Neuro 2a cells and L2 cells at an MOI of 0.01. Viral titre in cell supernatant were measured by plaque assay. Means with SD are shown ( $n = 3$ ). \*\*\*\* $P < 0.0001$ ; \*\*\* $P < 0.001$ ; \*\* $P < 0.01$ ; \* $P < 0.05$  (unpaired Student's  $t$ -test).

group was transferred to the unlabelled GpppA-RNA by activated MTase. As expected, while the N7-MTase activity of the WT nsp14 was set as 100%, the N7-MTase activity of the mutant nsp14 D330A and Y414A was very low, reaching 14% and 17%, respectively, but was significantly higher than the background value (Figure 1(B)), suggesting that the single amino acid substitution D330A and Y414A can partially abolish N7-MTase activity of MHV nsp14. Additionally, we expressed nsp14 of emerging SARS-CoV-2 and determined its N7-MTase activity. The result showed that SARS-CoV-2 nsp14 possesses strong N7-MTase activity (Figure 1(B)), which also indicates that N7-MTase is highly conserved among CoVs.

To further explore the details of these two mutations in terms of coronavirus replication and pathogenicity, we engineered and rescued two MHV N7-MTase mutant viruses, D330A and Y414A, and wild-type (WT) MHV using a vaccinia virus-based reverse genetic system. The rescued mutant viruses P0 were sequenced and it was confirmed that the designed mutation D330A and Y414A were introduced (data not shown). As Figure 1(C) shows, both of the N7-MTase mutant viruses exhibited smaller plaque morphologies compared to those of the WT viruses. Considering the genetic stability of the mutants during viral replication, we continuously passaged the mutant viruses P0 on Neuro 2a cells for 10 rounds and found that D330A and Y414A mutations

still remained, while no extra mutation was introduced within the nsp14 gene segment according to the sequencing results of P10 mutants (Figure 1(D)). P10 viruses were therefore used in latter experiments. The one-step growth curves of mutants in mammalian cell line Neuro 2a and L2 showed that the D330A mutant replicated slightly slower than the WT virus during the early stages (4–12 h), but peaked at similar levels to the WT virus. Meanwhile, the Y414A mutant showed a slightly reduced replication capacity in Neuro 2a cells but possessed similar replication kinetics to WT viruses in L2 cells (Figure 1(E)). Taken together, these results suggest that N7-MTase mutant coronaviruses harbouring a single amino acid substitution of D330A or Y414A are stable and slightly attenuated in vitro.

### **N7-MTase mutants are highly attenuated and change the delayed IFN-I production in mice**

MHV strain A59 (MHV-A59) can cause acute hepatitis or even death after intraperitoneal inoculation of 4–6-week-old C57BL/6 mice [29,30]. To compare the virulence and pathogenicity of the mutant and WT viruses in vivo, groups of 4-week-old male C57BL/6 mice were intrahepatically inoculated (i.h.) with  $2 \times 10^6$  PFU of mutant D330A, Y414A or WT MHV-A59. We then monitored the mice for body weight loss and clinical signs of disease and mortality daily (Figure 2(A)). At the early stage of infection ( $\leq 24$  h), mice infected with mutant D330A, Y414A or WT suffered a short-term body weight plateau with minor symptoms of illness. However, as the infection progressed, both D330A- and Y414A-infected mice started to gain weight slowly and their survival rate increased compared to WT-infected mice, which lost massive weight until death (Figure 2(B,C)). Furthermore, mice infected with the WT virus presented significantly higher levels of viral titres in the liver at 1, 2, 5 dpi, whereas the viral load of mice infected with D330A and Y414A could only be detected at 1 dpi and manifested as 68-fold and 350-fold decrease compared to WT virus-infected mice, respectively (Figure 2(D)). These results indicate that the mutant D330A and Y414A were sharply replication-limited and were quickly cleared by host animals.

Further examination of liver function and injury also revealed significant attenuation of N7-MTase mutants in mice. Both liver histopathological analysis and alanine aminotransferase (ALT) measurement showed that only minimal signs of disease occurred in mice after infection with the D330A and Y414A mutants at 1 dpi (Figure 2(E,F)). In contrast, mice inoculated with WT viruses maintained high levels of ALT from 1 to 5 dpi, which means that the liver damage was gradually exacerbated. These results were correlated with the greatest loss of body weight

(Figure 2(B)) and viral loads (Figure 2(D)). Moreover, as the viral infection persisted, fibrosis and the connective tissues became obvious in the liver of WT groups (Figure 2(F)), while the mock infection group and mutant groups did not show any lesions in the liver at 5 dpi (Figure 2(F)).

Having observed highly attenuated phenotypes of N7-MTase mutants, we next compared the IFN-I production induced by N7-MTase mutants and the WT virus. As Figure 2(G) shows, IFN- $\beta$  levels in the sera of D330A-infected and Y414A-infected mice accumulated from 8 hpi and peaked at 12 hpi, while the IFN- $\beta$  levels of WT-infected mice were significantly lower than N7-MTase mutants. At 24 hpi, mutant-infected mice gradually recovered from infection and the amount of IFN- $\beta$  also declined, whereas WT MHV replicated to higher titres and induced more IFN- $\beta$  to resist viral infection (Figure 2(D)). Similarly, higher *Ifnb* mRNA levels were induced in mouse bone marrow-derived dendritic cells (BMDCs) at 8 h after infection with mutant D330A (2.13-fold increase) and mutant Y414A (4.96-fold increase) compared to WT virus-infected mice (Figure 2(H)). These results are consistent with the reports that CoVs can delay IFN-I signalling, leading to elevated cytokine/chemokine levels at the late stage of infection after the viral titres peak [31,32]. Interestingly, our results showed that N7-MTase mutants could induce an earlier IFN-I production than the WT virus did in mice, which altered the delayed IFN-I production of CoVs.

### **N7-MTase mutants induced both humoral and cellular immune responses in mice**

Based on the attenuation of N7-MTase mutants in mice, we further evaluated the immunogenicity and protective efficacy of the mutants in mice to investigate the possibility of targeting viral N7-MTase to design live attenuated vaccines. For vaccination, groups of 4-week-old male C57BL/6 mice were subcutaneously (s.c.) inoculated with a dose of  $5 \times 10^5$  PFU mutant D330A, Y414A and WT MHV-A59, while DMEM was used as a mock control (Figure 3(A)). Mice were observed for 8 days for symptoms of infection. As expected, this mild inoculation method through the s.c. route did not cause a pathology in mice from both the mutant and WT groups. At 2 and 4 wpi, sera of animals were collected for evaluation of humoral immune responses. The results showed that MHV-specific IgG induced by N7-MTase mutants rapidly reached a comparative level to the WT virus as early as 14 dpi and this could be maintained until 28 dpi (Figure 3(B)). Furthermore, we determined the neutralizing antibody (NA) titres in the serum of immunized animals by PRNT<sub>50</sub> assay. As expected, the PRNT<sub>50</sub> values of virus-infected mice rapidly reached a significantly higher

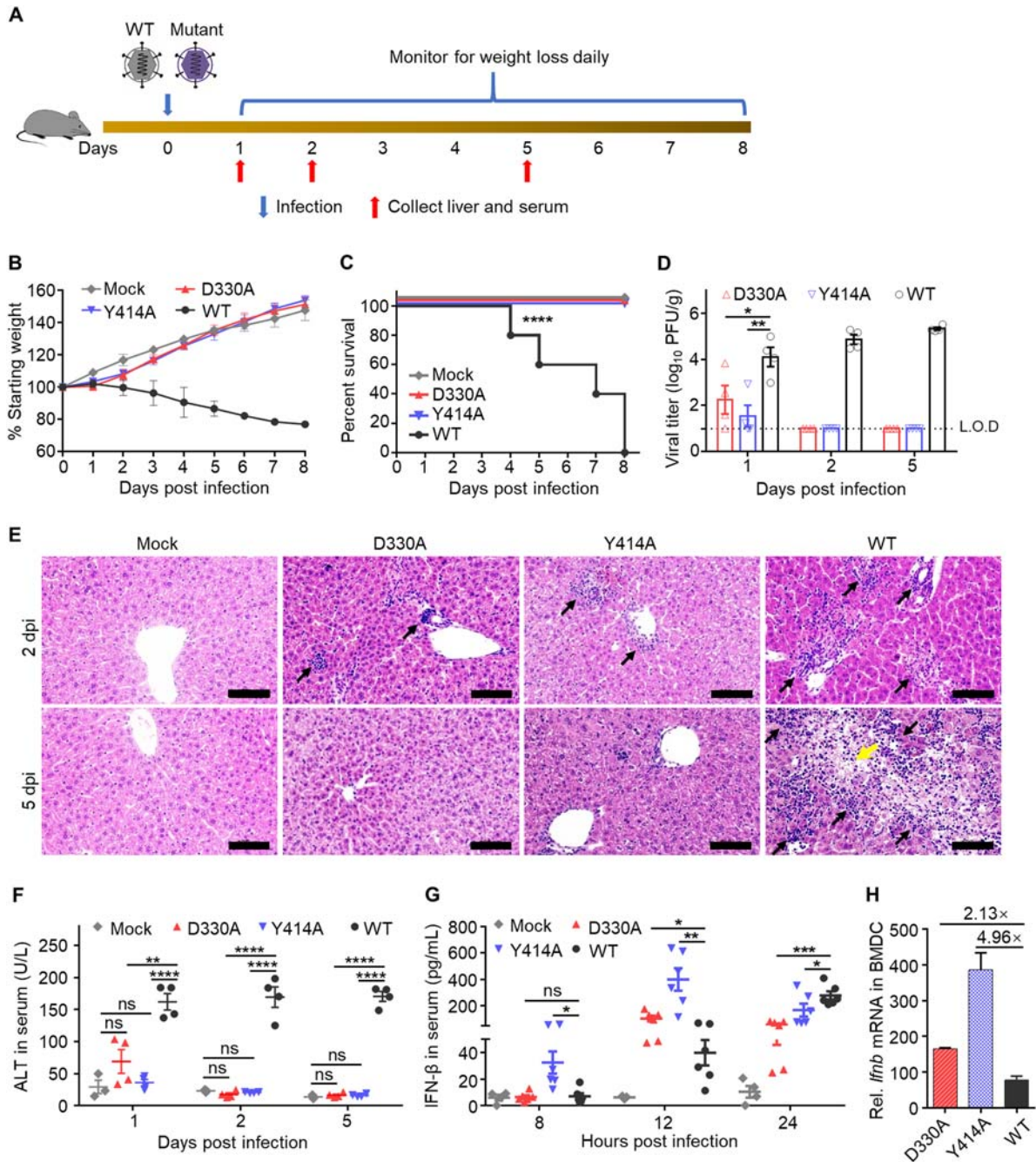


**Figure 2.** N7-MTase mutants are highly attenuated in vivo. (A) Scheme of infection. Four-week-old C57BL/6 male mice were i.h. infected with  $2 \times 10^6$  PFU N7-MTase mutants or WT virus, respectively. An equal volume of DMEM was injected as a mock control. Mice were monitored for 8 days for (B) body weight changes ( $n = 5$ ) and (C) survival ( $n = 5$ ). Means with SD are shown. (D) Viral loads in liver at 1, 2, 5 dpi were measured by plaque assay. Means with SEM are shown ( $n = 4$ ). L.O.D: Limit of detection. (E) Liver histopathological changes of mice. The black arrow indicates inflammatory cell infiltration; the yellow arrow indicates liver fibrosis. Scale bar, 100  $\mu$ m. (F) ALT levels in mice sera. Liver damage was evaluated by measuring the ALT level in serum. Means with SEM are shown ( $n = 3-4$ ). (G) The IFN- $\beta$  level in mice sera was detected by ELISA at 8, 12, 24 hpi. Means with SEM are shown ( $n = 3-6$ ). (H) The relative *Ifnb* mRNA level in BMDCs was detected at 8 hpi. Means with SD are shown ( $n = 3$ ). \*\*\*\* $P < 0.0001$ ; \*\*\* $P < 0.001$ ; \*\* $P < 0.01$ ; \* $P < 0.05$ ; ns, not significant,  $P > 0.05$  (unpaired Student's *t*-test).

level than the mock group at both two and four weeks after immunization (Figure 3(C)). Although strong humoral immune responses were induced, the IgE induced by viruses was as low as the mock group (data not shown), suggesting that N7-MTase mutants did not mediate an anaphylactic reaction. Surprisingly, continuous neutralizing antibody monitoring showed that the NA could last for at least 48 weeks

in serum (Figure 3(D)). These results indicated that a robust and long-term humoral immune response was activated after immunization with attenuated N7-MTase mutants in mice.

While antibodies are crucial to reducing the viral load by binding and neutralizing virus particles, T cell responses are also necessary for efficient viral clearance [33-35]. To detect the type and level of T-

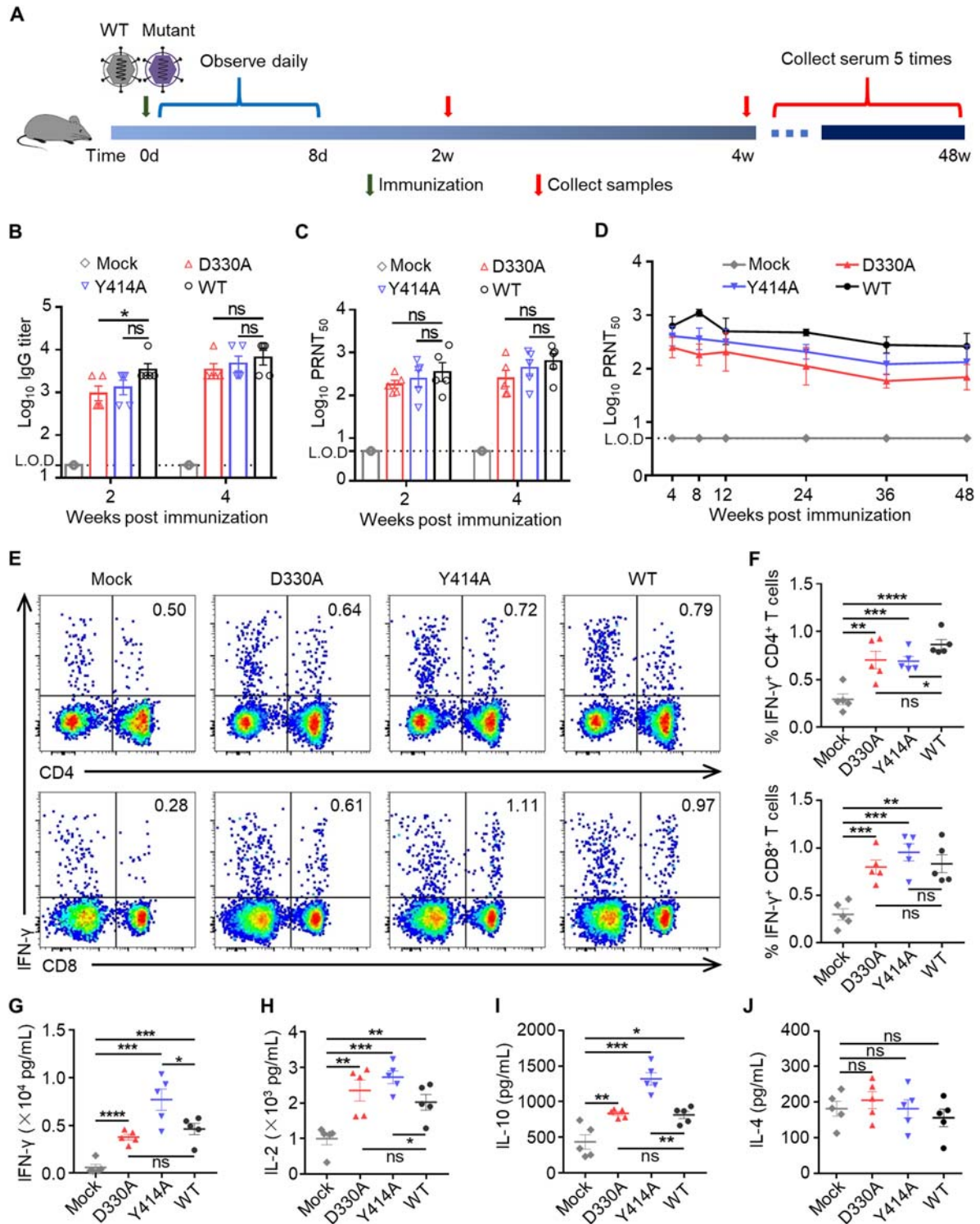


**Figure 3.** MHV nsp14 N7-MTase mutants induced both humoral and cellular immune responses in mice. (A) Scheme of immunization. Four-week-old C57BL/6 mice were s.c. immunized with  $5 \times 10^5$  PFU N7-MTase mutants or WT viruses. Sera were collected at 2 and 4 wpi. At 4 wpi, mouse spleens were harvested. (B) Virus-specific IgG titre in mice serum. Sera were 5-fold serial-diluted and the IgG titre was then measured by ELISA. Means with SEM are shown ( $n = 5$ ). (C) Neutralizing antibody titre in sera of mice. To neutralize the antibody titre, sera were 2-fold serial-diluted to the PRNT<sub>50</sub> test. Means with SEM are shown ( $n = 5$ ). (D) Virus-specific neutralizing antibodies can exist for at least 48 weeks in the sera of immunized animals. Means with SEM are shown ( $n = 3 \sim 5$ ). (E) Spleens of immunized mice were collected at 4 wpi. Single splenocytes were cultured ex vivo and stimulated with WT MHV for 24 h, after which they were stained for markers (IFN- $\gamma$ , CD3, CD4 or CD8). The T-cells were gated and the percentages of (F) IFN- $\gamma$ <sup>+</sup> CD4<sup>+</sup> cells and (G) IFN- $\gamma$ <sup>+</sup> CD8<sup>+</sup> cells are shown. Means with SEM are shown ( $n = 5$ ). (G), (H), (I), and (J) Total splenocyte supernatant from the ex vivo culture was collected 48 h after WT MHV stimulation, and IFN- $\gamma$ , IL-2, IL-10, and IL-4 production were measured by ELISA. Data are presented as means  $\pm$  S.E.M. Means with SEM are shown ( $n = 5$ ). \*\*\*\* $P < 0.0001$ ; \*\*\* $P < 0.001$ ; \*\* $P < 0.01$ ; \* $P < 0.05$ ; ns, not significant,  $P > 0.05$  (unpaired Student's  $t$ -test).

cell responses, we immunized C57BL/6 mice with both N7-mutants and WT virus, as mentioned above. The spleens of mice were harvested at 4 wpi for restimulation *in vitro*. We then detected cytokines production through an intracellular cytokine staining assay (ICS) and ELISA. The results showed that CD4<sup>+</sup> and CD8<sup>+</sup> T cells of both WT- and mutant-immunized mice had a higher interferon (IFN)- $\gamma$  response than the mock-immunized group after re-stimulation with WT MHV-A59 (Figure 3(E-G)). Notably, the strength of the T cell response was similar in the D330A, Y414A, and WT groups. Furthermore, total splenocytes induced more Th1 cytokine IFN- $\gamma$ , interleukin (IL)-2 and Th2 cytokine IL-10 (Figure 3(H,I)) than the mock group. The splenocytes of mice immunized with Y414A produced higher levels of cytokines than cells immunized with the WT virus (IFN- $\gamma$ ,  $P = 0.0399$ ; IL-2,  $P = 0.0388$ ; IL-10,  $P = 0.0010$ ). Taken together, our findings show that coronavirus N7-MTase mutants can induce long-lasting humoral responses, as well as robust CD4<sup>+</sup> and CD8<sup>+</sup> T cell responses in mice.

#### **Immunization with N7-MTase mutants protected C57BL/6 mice from death**

To determine the protective efficacy of N7-MTase mutants, we immunized mice as mentioned above, and then they were challenged with WT MHV-A59 at a lethal dose of  $2 \times 10^7$  PFU by the i.h. route (Figure 4(A)). Four of the five mock-immunized mice showed drastic weight loss and died within eight days after the challenge, whereas all the virus-immunized mice survived the lethal challenge (Figure 4(B,C)). Moreover, viral load detection showed that MHV viruses replicated at a minimal level in the liver of all virus-immunized mice at 2 dpi. At 5 dpi, viruses were not detected in the liver of virus-immunized mice, whereas a significantly higher viral titre was maintained in the liver of mock-immunized mice (Figure 4(D)). Similar results were shown in the ALT assay and liver histopathological analysis (Figure 4(E,F)), in which no liver damage was observed after challenge with high pathogenic WT virus. Thus, these results indicated that a single dose of N7-MTase mutant immunization could provide full protection against lethal challenges.

#### **Discussion**

Since the first coronavirus was documented in 1931, an increasing number of CoVs have been discovered from different contagious diseases, which have great impacts on human health and the economy. Although significant progress has been made on the origin of CoV, cross-species transmission, replication, virus-host interactions, and pathogenesis, there is still lack

of effective therapeutic options for CoV infection [3]. Thus, vaccination remains the most promising method with which to prevent CoV infection.

Nowadays, available strategies to develop coronavirus vaccines include live attenuated vaccines (LAV), inactivated vaccines, recombinant viral vector vaccines, subunit protein vaccines, DNA vaccines, and RNA vaccines, among others [36]. LAVs generally consist of weakened versions of the pathogens, which can defectively replicate but closely mimic the protective immunity that the live pathogen induces in hosts, hence even a single immunization can elicit strong and long-term adapted immune responses [37]. Successful experience in CoV vaccine development started with livestock CoV prevention in the last century. Live attenuated IBV vaccines and live attenuated TGEV vaccines, which are usually produced by serially passaging pathogenic strains in cells or animals, are most commonly used in all sectors of the poultry and pork industry [38,39]. However, one main concern about LAVs is that there is a risk of reversion to virulence due to their unclear attenuation mechanism and the possibility of their recombination with other circulating CoVs. By contrast, other kinds of vaccines are relatively safer, but have multiple shortcomings such as weak immunogenicity, lack of cytotoxic T lymphocyte (CTL) responses mediated by CD8<sup>+</sup> T cells, the need for several booster immunization, and higher costs. Considering both the cost and effectiveness, a more safe, affordable, and fully protective LAV would be most desirable.

In this proof-of-concept study, we targeted the core functional domain of CoV N7-MTase and mutated two conserved key activity residues at positions D330 and Y414 of MHV nsp14 to rationally design a live attenuated coronavirus vaccine by the reverse genetic system. In contrast to the traditional method used to develop LAVs by passaging WT viruses on cell lines or animals, this strategy, based on the reverse genetic system, has the advantage of precisely introducing the specific mutation to attenuate the virus [40]. Our results showed that the N7-MTase mutants MHV D330A and Y414A were replicative and stable in the cell culture, which indicates that it would be cheap and easy to prepare these mutants as LAVs in a short time. Moreover, D330A and Y414A can be rapidly cleared within 2 dpi after infecting mice, indicating that these mutants are highly attenuated and safe (Figure 2). More importantly, an N7-MTase live attenuated vaccine can induce long-lasting humoral immune responses mediated by neutralizing antibodies and produce robust CD4<sup>+</sup> and CD8<sup>+</sup> T-cell immune responses (Figure 3), which are required for viral clearance from a host. However, considering the susceptibility of CoVs to immunocompromised individuals, further study or optimization of the N7-MTase mutant may be needed.

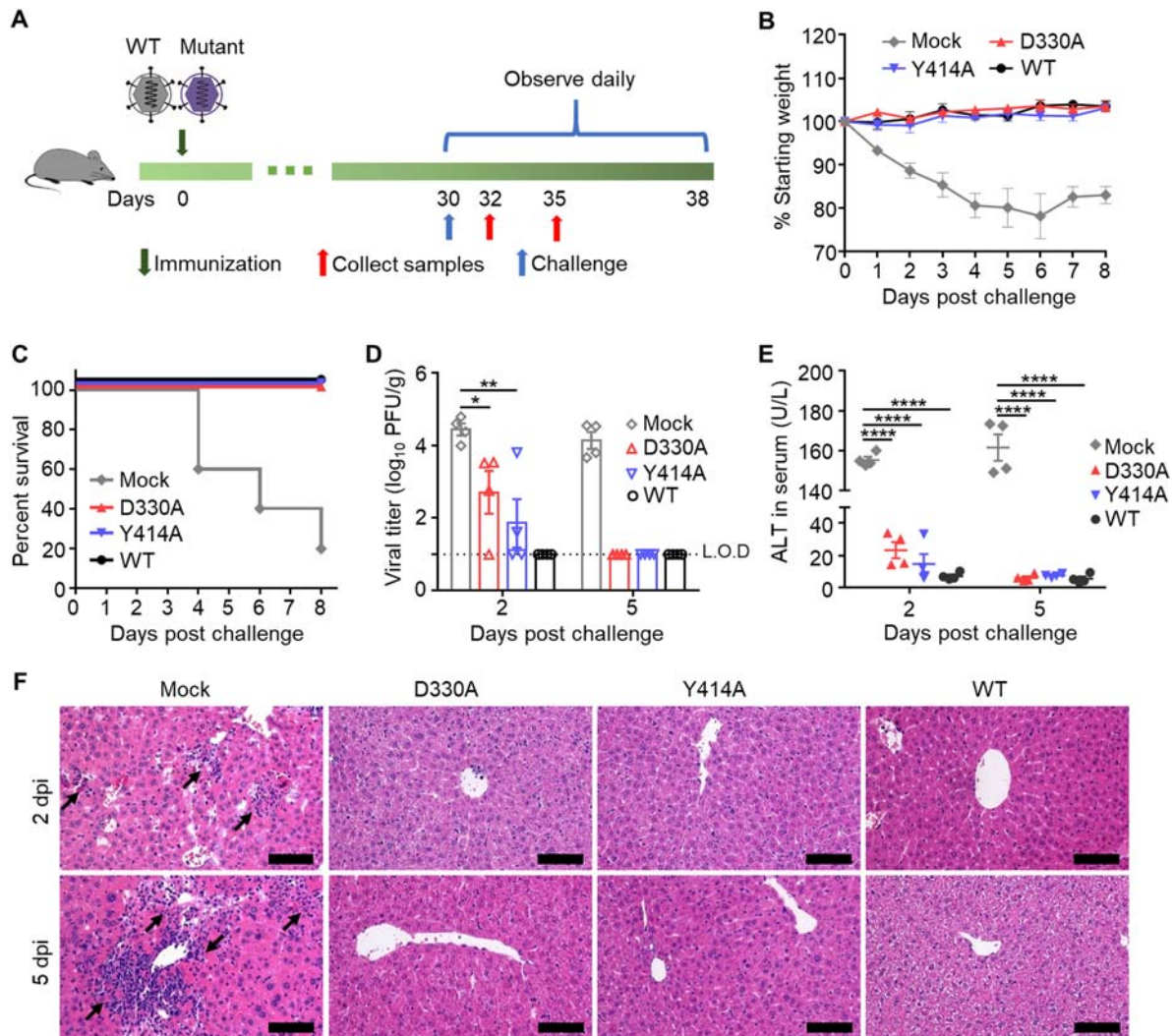


**Figure 4.** MHV nsp14 N7-MTase mutants immunization protects mice from death after challenge. (A) Scheme of challenge of C57BL/6 mice. Four-week-old C57BL/6 mice were immunized with  $5 \times 10^5$  PFU D330A, Y414A, while the WT virus and DMEM were used as positive and mock control, respectively. At 30 dpi, animals were i.h. challenged with a high lethal dose of  $2 \times 10^7$  PFU WT MHV. (B) Body weight change. Means with SD are shown ( $n = 5$ ). (C) Survival 8 days after challenge ( $n = 5$ ). (D) Viral loads in livers were measured by plaque assay at 2- and 5- days post challenge. Means with SEM are shown ( $n = 4$ ). L.O.D.: Limit of detection. (E) Liver damage was evaluated by measuring the ALT level in sera. Means with SEM are shown ( $n = 4$ ). (F) Liver histological changes of mice. Black arrows indicate inflammatory cell infiltration. Scale bar, 100  $\mu$ m. \*\*\*\* $P < 0.0001$ ; \*\* $P < 0.01$ ; \* $P < 0.05$  (unpaired Student's *t*-test).

During viral infection, IFN-I, which can be induced by many kinds of pattern recognition receptors (PRRs), plays an important role in initiating innate immune responses, activating the adaptive immune system and promoting the development of antigen-specific T and B cell responses [41]. Therefore, some ligands of PRRs are used as novel adjuvants to overcome the weak immunogenicity of non-LAVs vaccines and to change the immune response patterns [37,42]. Our results showed that N7-MTase mutants, especially Y414A, can induce higher IFN-I production at the early stage of infection without any adjuvants (Figure 2), and can build strong neutralizing antibody responses and cellular immune responses after immunization (Figure 3). Notably, wild-type or natural CoVs are reported to delay IFN-I signalling [31,43,44], but the mechanism is not yet fully

understood. *Case et al.* reported that N7-MTase deficient MHV (G332A) impairs viral replication, enhances sensitivity to the innate immune response, and reduces viral RNA translation efficiency in cell culture. What's more, another group showed that N7-MTase deficient PEDV (D350A), which belongs to *Alphacoronavirus*, can induce higher IFN-I and IFN-III responses in cell culture [45,46]. Both these two and our studies indicated that CoV nsp14 N7-MTase contributes to the IFN-I delay during CoV infections. Since N7-MTase is the key enzyme to form the mature 5'-cap structures of the CoV RNAs, we speculate that the earlier IFN-I production induced by N7-MTase deficient CoVs is related to the large amount of unmethylated CoV RNAs, which may be recognized by host's PRRs like Mda5 or Toll-like receptors [22]. IFN-I is secreted and signals through

the type I interferon receptor (IFNAR), followed by the establishment of host cell antiviral state, which might be the reason for the rapid clearance of D330A and Y414A in vivo. However, the detailed mechanism mediating this phenotype warrants further study.

In conclusion, we have demonstrated the feasibility of adopting the highly attenuated recombinant N7-MTase mutant as a potential coronavirus live vaccine approach by in vitro and in vivo characterization of the N7-MTase activity of MHV nsp14. This vaccine approach needs further development, especially considering the great need for a low-cost but high-efficacy vaccine for a variety of infectious diseases caused by CoVs in the livestock industry. Meanwhile, this kind of live attenuated CoVs lacking N7-MTase may have the potential to develop into vaccine strains, which can be used to prepare inactivated vaccines (such as current SARS-CoV-2 inactivated vaccines) on account of their reduced biosafety risks. What's more, this rational design approach may be applicable to other viruses with defined N7-MTase activity for potential vaccine development.

### Acknowledgements

We are grateful to Prof. Chang Guohui, State Key Laboratory of Pathogen and Biosecurity, Beijing, China, for his great support to this work. We are grateful to Beijing Taikang Yicai Foundation for their great support to this work.

### Disclosure statement

No potential conflict of interest was reported by the author(s).

### Funding

This study was supported by grants from the National Science and Technology Major Project [grant number 2018YFA0900801], National Science Foundation of China [grant number 32041007], Fundamental Research Funds for the Central Universities [grant number 2042021kf0220], the Advanced Customer Cultivation Project of Wuhan National Biosafety Laboratory [grant number 2021ACCP-MS10] and Special Fund for COVID-19 Research of Wuhan University.

### Data availability

All data obtained for this study is included in the article.

### Authors contributions

Y.C., Z.Z. and Q.L. conceived the study and designed the experiments. Z.Z., Q.L. and Y.S. performed the experiments. J.L., J.L., R.P., L.C., X.C., Y.L. and Y.Z. assisted with the experiments. Z.Z. and Q.L. analysed the figures. Z.Z. wrote the initial draft of the

manuscript. Q.L., L.Z. and Y.C. revised the manuscript. All others read and commented on the manuscript.

### ORCID

Zhen Zhang  <http://orcid.org/0000-0002-4156-1993>

Qianyun Liu  <http://orcid.org/0000-0002-9179-4867>

Li Zhou  <http://orcid.org/0000-0002-6736-0057>

Ke Lan  <http://orcid.org/0000-0002-0384-8598>

Yu Chen  <http://orcid.org/0000-0003-1300-4652>

### References

- [1] Chen Y, Liu Q, Guo D. Emerging coronaviruses: genome structure, replication, and pathogenesis. *J Med Virol.* 2020 Oct;92(10):2249.
- [2] Coronaviridae Study Group of the International Committee on Taxonomy of V. The species severe acute respiratory syndrome-related coronavirus: classifying 2019-nCoV and naming it SARS-CoV-2. *Nat Microbiol.* 2020 Apr;5(4):536–544.
- [3] V'Kovski P, Kratzel A, Steiner S, et al. Coronavirus biology and replication: implications for SARS-CoV-2. *Nat Rev Microbiol.* 2021 Mar;19(3):155–170.
- [4] Lin SY, Chen HW. Infectious bronchitis virus variants: molecular analysis and pathogenicity investigation. *Int J Mol Sci.* 2017 Sep 22;18(10).
- [5] Wang Q, Vlasova AN, Kenney SP, et al. Emerging and re-emerging coronaviruses in pigs. *Curr Opin Virol.* 2019 Feb;34:39–49.
- [6] Zhou P, Fan H, Lan T, et al. Fatal swine acute diarrhoea syndrome caused by an HKU2-related coronavirus of bat origin. *Nature.* 2018 Apr;556(7700):255–258.
- [7] Bender SJ, Weiss SR. Pathogenesis of murine coronavirus in the central nervous system. *J Neuroimmune Pharmacol: Off J Soc NeuroImmune Pharmacol.* 2010 Sep;5(3):336–354.
- [8] Su S, Wong G, Shi W, et al. Epidemiology, genetic recombination, and pathogenesis of coronaviruses. *Trends Microbiol.* 2016 Jun;24(6):490–502.
- [9] Zhong NS, Zheng BJ, Li YM, et al. Epidemiology and cause of severe acute respiratory syndrome (SARS) in guangdong, people's Republic of China, in February, 2003. *Lancet.* 2003 Oct 25;362(9393):1353–1358.
- [10] Zumla A, Hui DS, Perlman S. Middle East respiratory syndrome. *Lancet.* 2015 Sep 5;386(9997):995–1007.
- [11] Zhou P, Yang XL, Wang XG, et al. A pneumonia outbreak associated with a new coronavirus of probable bat origin. *Nature.* 2020 Mar;579(7798):270–273.
- [12] Chen L, Liu W, Zhang Q, et al. RNA based mNGS approach identifies a novel human coronavirus from two individual pneumonia cases in 2019 Wuhan outbreak. *Emerg Microbes Infect.* 2020;9(1):313–319.
- [13] Zhu N, Zhang D, Wang W, et al. A novel coronavirus from patients with pneumonia in China, 2019. *N Engl J Med.* 2020 Feb 20;382(8):727–733.
- [14] Hu B, Guo H, Zhou P, et al. Characteristics of SARS-CoV-2 and COVID-19. *Nat Rev Microbiol.* 2021 Mar;19(3):141–154.
- [15] Huang C, Wang Y, Li X, et al. Clinical features of patients infected with 2019 novel coronavirus in Wuhan, China. *Lancet.* 2020 Feb 15;395(10223):497–506.

- [16] Gosert R, Kanjanahaluethai A, Egger D, et al. RNA replication of mouse hepatitis virus takes place at double-membrane vesicles. *J Virol.* 2002 Apr;76(8):3697–3708.
- [17] Denison MR, Perlman S. Translation and processing of mouse hepatitis virus virion RNA in a cell-free system. *J Virol.* 1986 Oct;60(1):12–18.
- [18] Yan L, Ge J, Zheng L, et al. Cryo-EM structure of an extended SARS-CoV-2 replication and transcription complex reveals an intermediate State in Cap synthesis. *Cell.* 2021 Jan 7;184(1):184–193 e10.
- [19] Sawicki SG, Sawicki DL. Coronaviruses use discontinuous extension for synthesis of subgenome-length negative strands. *Adv Exp Med Biol.* 1995;380:499–506.
- [20] Wang D, Jiang A, Feng J, et al. The SARS-CoV-2 subgenome landscape and its novel regulatory features. *Mol Cell.* 2021 May 20;81(10):2135–2147 e5.
- [21] Chen Y, Guo D. Molecular mechanisms of coronavirus RNA capping and methylation. *Virologica Sinica.* 2016 Feb;31(1):3–11.
- [22] Zust R, Cervantes-Barragan L, Habjan M, et al. Ribose 2'-O-methylation provides a molecular signature for the distinction of self and non-self mRNA dependent on the RNA sensor Mda5. *Nat Immunol.* 2011 Feb;12(2):137–143.
- [23] Chen Y, Cai H, Pan J, et al. Functional screen reveals SARS coronavirus nonstructural protein nsp14 as a novel cap N7 methyltransferase. *Proc Natl Acad Sci USA.* 2009 Mar 3;106(9):3484–3489.
- [24] Chen Y, Tao J, Sun Y, et al. Structure-function analysis of severe acute respiratory syndrome coronavirus RNA cap guanine-N7-methyltransferase. *J Virol.* 2013 Jun;87(11):6296–6305.
- [25] Sun Y, Wang Z, Tao J, et al. Yeast-based assays for the high-throughput screening of inhibitors of coronavirus RNA cap guanine-N7-methyltransferase. *Antiviral Res.* 2014 Apr;104:156–164.
- [26] Coley SE, Lavi E, Sawicki SG, et al. Recombinant mouse hepatitis virus strain A59 from cloned, full-length cDNA replicates to high titers in vitro and is fully pathogenic in vivo. *J Virol.* 2005 Mar;79(5):3097–3106.
- [27] Lei L, Ying S, Baojun L, et al. Attenuation of mouse hepatitis virus by deletion of the LLRKxGxKG region of Nsp1. *PLoS one.* 2013;8(4):e61166.
- [28] Minskaia E, Hertzog T, Gorbalenya AE, et al. Discovery of an RNA virus 3'->5' exoribonuclease that is critically involved in coronavirus RNA synthesis. *Proc Natl Acad Sci USA.* 2006 Mar 28;103(13):5108–5113.
- [29] Lavi E, Gildea DH, Highkin MK, et al. The organ tropism of mouse hepatitis virus A59 in mice is dependent on dose and route of inoculation. *Lab Anim Sci.* 1986 Apr;36(2):130–135.
- [30] Wang Y, Sun Y, Wu A, et al. Coronavirus nsp10/nsp16 methyltransferase can be targeted by nsp10-derived peptide in vitro and in vivo to reduce replication and pathogenesis. *J Virol.* 2015 Aug;89(16):8416–8427.
- [31] Lei X, Dong X, Ma R, et al. Activation and evasion of type I interferon responses by SARS-CoV-2. *Nat Commun.* 2020 Jul 30;11(1):3810.
- [32] Kindler E, Thiel V. SARS-CoV and IFN: too little, Too late. *Cell Host Microbe.* 2016 Feb 10;19(2):139–141.
- [33] Williamson JS, Stohlman SA. Effective clearance of mouse hepatitis virus from the central nervous system requires both CD4+ and CD8+ T cells. *J Virol.* 1990 Sep;64(9):4589–4592.
- [34] Grifoni A, Weiskopf D, Ramirez SI, et al. Targets of T cell responses to SARS-CoV-2 coronavirus in humans with COVID-19 disease and unexposed individuals. *Cell.* 2020 Jun 25;181(7):1489–1501 e15.
- [35] Le Bert N, Tan AT, Kunasegaran K, et al. SARS-CoV-2-specific T cell immunity in cases of COVID-19 and SARS, and uninfected controls. *Nature.* 2020 Aug;584(7821):457–462.
- [36] Krammer F. SARS-CoV-2 vaccines in development. *Nature.* 2020 Oct;586(7830):516–527.
- [37] Pulendran B, Ahmed R. Immunological mechanisms of vaccination. *Nat Immunol.* 2011 Jun;12(6):509–517.
- [38] Jordan B. Vaccination against infectious bronchitis virus: A continuous challenge. *Vet Microbiol.* 2017 Jul;206:137–143.
- [39] Turlewicz-Podbielska H, Pomorska-Mol M. Porcine coronaviruses: overview of the State of the Art. *Virologica Sinica.* 2021 Mar 15; 1–19.
- [40] Stobart CC, Moore ML. RNA virus reverse genetics and vaccine design. *Viruses.* 2014 Jun 25;6(7):2531–2550.
- [41] Ivashkiv LB, Donlin LT. Regulation of type I interferon responses. *Nat Rev Immunol.* 2014 Jan;14(1):36–49.
- [42] Gutjahr A, Papagno L, Nicoli F, et al. The STING ligand cGAMP potentiates the efficacy of vaccine-induced CD8+ T cells. *JCI Insight.* 2019 Apr 4;4(7).
- [43] Rose KM, Weiss SR. Murine coronavirus cell type dependent interaction with the type I interferon response. *Viruses.* 2009 Dec 1;1(3):689–712.
- [44] Channappanavar R, Fehr AR, Vijay R, et al. Dysregulated type I interferon and inflammatory monocyte-macrophage responses cause lethal pneumonia in SARS-CoV-infected mice. *Cell Host Microbe.* 2016 Feb 10;19(2):181–193.
- [45] Case JB, Ashbrook AW, Dermody TS, et al. Mutagenesis of S-adenosyl-l-methionine-binding residues in coronavirus nsp14 N7-methyltransferase demonstrates differing requirements for genome translation and resistance to innate immunity. *J Virol.* 2016 Aug 15;90(16):7248–7256.
- [46] Lu Y, Cai H, Lu M, et al. Porcine epidemic diarrhea virus deficient in RNA Cap guanine-N-7 methylation is attenuated and induces higher type I and III interferon responses. *J Virol.* 2020 Jul 30;94(16).